Proceedings of ISSS-6 (2001): 1–4 © Copernicus Gesellschaft 2001

ISSS–6

Tests and limits of Vlasov code simulations and its application to null-helicity and co-helicity reconnection

T. Wiegelmann[1], **T. Neukirch**[1], **and J. Büchner**[2]

[1]School of Mathematics and Statistics, University of St. Andrews, St. Andrews, KY16 9SS, United Kingdom
[2]Max-Planck-Institut für Aeronomie, Max-Planck-Str. 2, 37191 Katlenburg-Lindau, Germany

Abstract. Magnetic reconnection is an important process in many space plasmas (e.g. geomagnetic substorms, coronal mass ejections). The large scale structure of these phenomena is usually described within MHD. Reconnection requires a non ideal region (resistivity) in the plasma. The cause of a non ideal behaviour in localized regions could for example be anomalous resistivity in thin current sheets. The formation of these thin current sheets can be understand within the framework of MHD. The further evolution of the current sheets cannot be investigated with MHD, because the sheet width becomes comparable with kinetic scales like the ion gyro radius and kinetic effects have to be taken into account. For many space plasmas, the kinetic processes are collisionless and can thus be described by the Vlasov equation. A code to solve the Vlasov equation has been developed and we report first results obtained with the code. To test the accuracy and limits of our code we carry out several consistency checks, which can be compared with analytic results, in particular phase mixing and Landau damping. We also apply our Vlasov code to collisionless magnetic reconnection in the magnetospheric plasma sheet and at the magnetopause.

1 Introduction

Magnetic reconnection caused by thin current sheets plays an important role for the dynamics of many space plasma. Thin current sheets occur for example at the magnetopause and prior to a substorm in the magnetospheric plasma sheet.

The paper is organized as follows. In Sect. 2 we present time-dependent solutions of the force free Vlasov equation, where an initial inhomogenity is damped by phase mixing. In Sect. 3 we compare the analytic and numeric results for Landau damping. In Sect. 4 we apply our Vlasov code to null-helicity and co-helicity reconnection.

We use the following symbols for electron thermal velocity $v_{Te} = \sqrt{k_B T_e/M_e}$, electron plasma frequency $\Omega_{pe} = \sqrt{4\pi n q_e^2/M_e}$ and electron Debye length $\Lambda_{De} = \sqrt{k_B T_e/(4\pi n q_e^2)}$. Useful abbreviations are $a = M_e/(2\ k_B\ T_e) = 1/(2\ v_{Te}^2)$, $k_1 = 2\pi k/L$, $c_1 = \sqrt{M_e/(2\pi k_B T_e)}$.

Correspondence to: T. Wiegelmann (tw@mcs.st-and.ac.uk)

2 Phase mixing

As a first step we investigate the one-one-dimensional (in configuration space and velocity space, $f = f(x, v, t)$) force free Vlasov equation.

$$\frac{\partial f}{\partial t} + v \cdot \frac{\partial f}{\partial x} = 0$$

We find the exact solution of this equation with help of the method of characteristics as:

$$f(x, v, t) = f(x - v\,t, v, 0)$$

As initial distribution we choose a homogeneous, isothermal Maxwellian distribution with a periodic perturbation:

$$f(x, v, 0) = c_1 \cdot [n_0 + \epsilon_1 \cdot \sin(k_1 x)] \cdot \exp(-a v^2)$$

which leads us to the time dependent solution

$$f(x, v, t) = c_1 \cdot [n_0 + \epsilon_1 \cdot \sin(k_1 (x - v\,t))] \cdot \exp(-a v^2)$$

(Figure 4 shows the comparison of the exact solution with numeric solutions.) The particle density ($n = \int_{-\infty}^{\infty} f dv$) is given by:

$$n(x, t) = c_1 \sqrt{\frac{\pi}{a}} \cdot \left[n_0 + \epsilon_1 \exp\left(-\frac{k_1^2\, t^2}{4\, a} \right)\ \sin(k_1 x) \right]$$

where the integration over the velocity space has been carried out from $-\infty$ to ∞. In a numerical code, with a finite extent of the numerical box in the velocity space this is not possible and one has a finite velocity space (usual several thermal velocities). If $v_{\max}$ is normalized by thermal velocities the

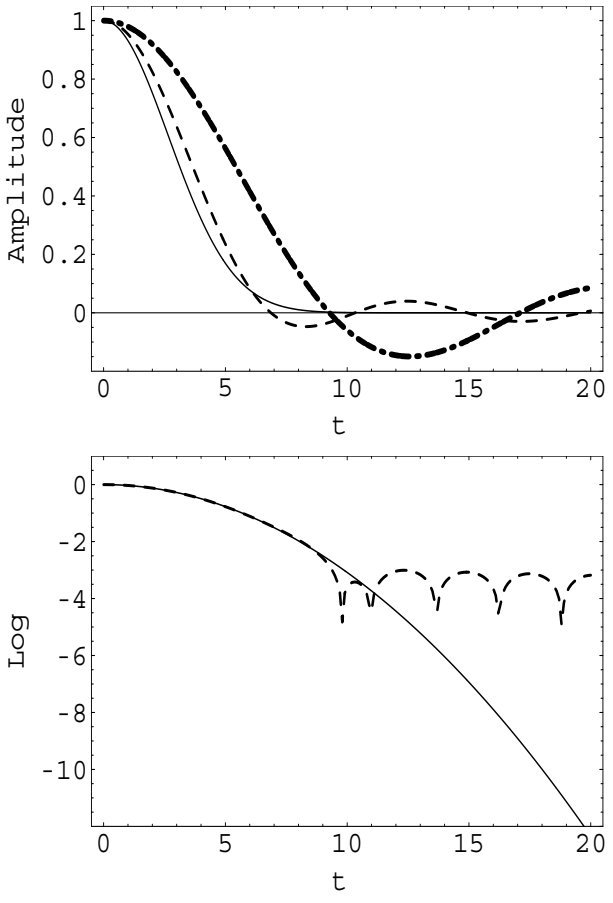

Fig. 1. Time evolution of the density perturbation amplitude. Upper panel shows the amplitude for $v_{\max} = \infty$ (solid line), $v_{\max} = 3\,v_{Te}$ (dashed line) and $v_{\max} = 1\,v_{Te}$ (dashdotted line). The lower panel shows the logarithm of the amplitude for $v_{\max} = \infty$ (solid line) and $v_{\max} = 10\,v_{Te}$ (dashdotted line).

term $\exp\left(-k_1^2\,t^2/(4\,a)\right)$ in the previous formula has to be replaced by:

$$\frac{\left(\mathrm{Erf}(\frac{-i\,k_1\,t+\sqrt{2}\,a\,\sqrt{\frac{v_{\max}}{a}}}{2\,\sqrt{a}}) + i\,\mathrm{Erfi}(\frac{k_1\,t-i\,\sqrt{2}\,a\,\sqrt{\frac{v_{\max}}{a}}}{2\,\sqrt{a}})\right)}{2\,e^{\frac{k_1{}^2\,t^2}{4\,a}}}$$

While the exact theory (infinite velocity space) predicts an exponential (with t^2) decreasing of inhomogenities due to phase mixing, a finite velocity space leads to an additional oscillatory part in the density evolution. Figure 1 shows the analytic solutions for the time evolution of the density perturbation amplitude for several velocity space size and Fig. 2 the corresponding numerical solutions with different size and resolution of the phase space.

3 Landau damping

Here we integrate the electron Vlasov equation and use the ions as background to investigate electrostatic phenomena. An electrostatic perturbation in a cold plasma oscillates with

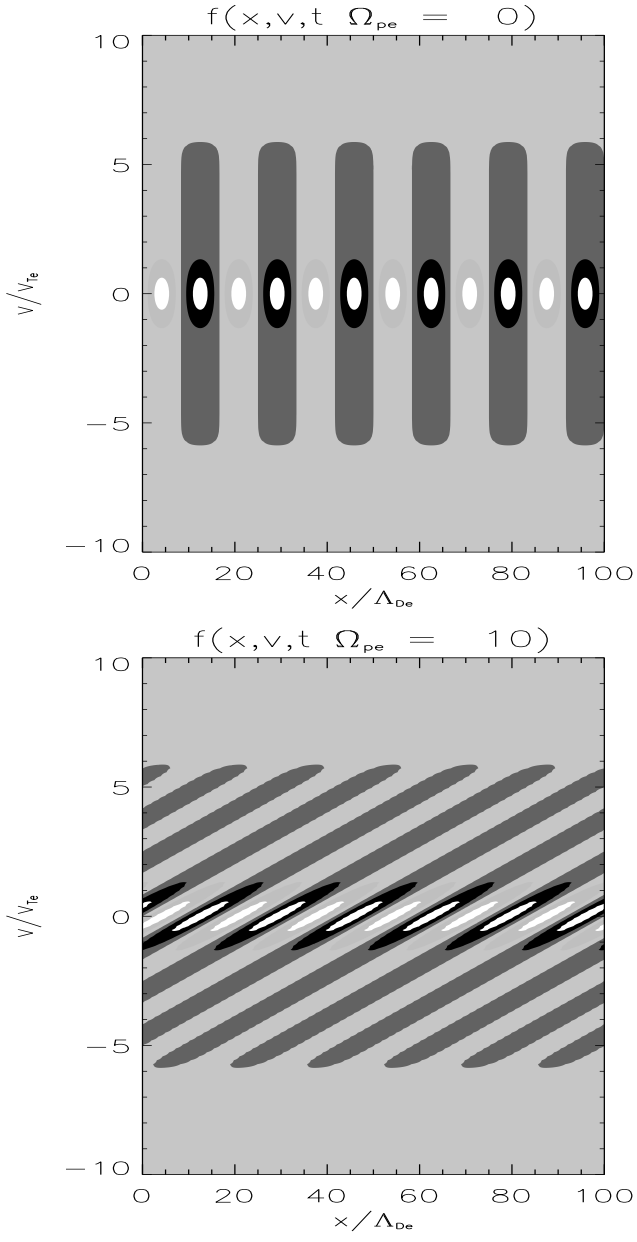

Fig. 2. Evolution of the phase space for a force free plasma. (only perturbation, background removed). The upper panel corresponds to the initial distribution and the lower panel after $t \cdot \Omega_{pi} = 10$ after phase mixing has occurred.

the plasma frequency $\Omega_r = \Omega_{pe}$. In a warm plasma the Langmuir oscillations are weakly damped due to Landau damping $\phi(x,t) = \phi_1 \exp[i\,(k\,x - \Omega_r\,t)]\,\exp(\Omega_i\,t)$. We get the simplified dispersion relation (Krall and Trivelpiece, 1986; Spatschek, 1990)

$$\Omega_r = \Omega_{pe}\left(1 + 1.5 k^2 \Lambda_{De}^2\right)$$

$$\Omega_i = -\sqrt{\frac{\pi}{8}}\,\frac{\Omega_{pe}}{|k^3\,\Lambda_{De}^3|}\,\exp\left(-\left(\frac{1}{2\,k^2\,\Lambda_{De}^2} + 1.5\right)\right)$$

Please note that this simplified form is only valid for $\Omega_r/(k\,v_{Te}) \gg 1$, $k\Lambda_{De} \ll 1$, $\Omega_i/\Omega_r \ll 1$ and $L \gg 1/k$.

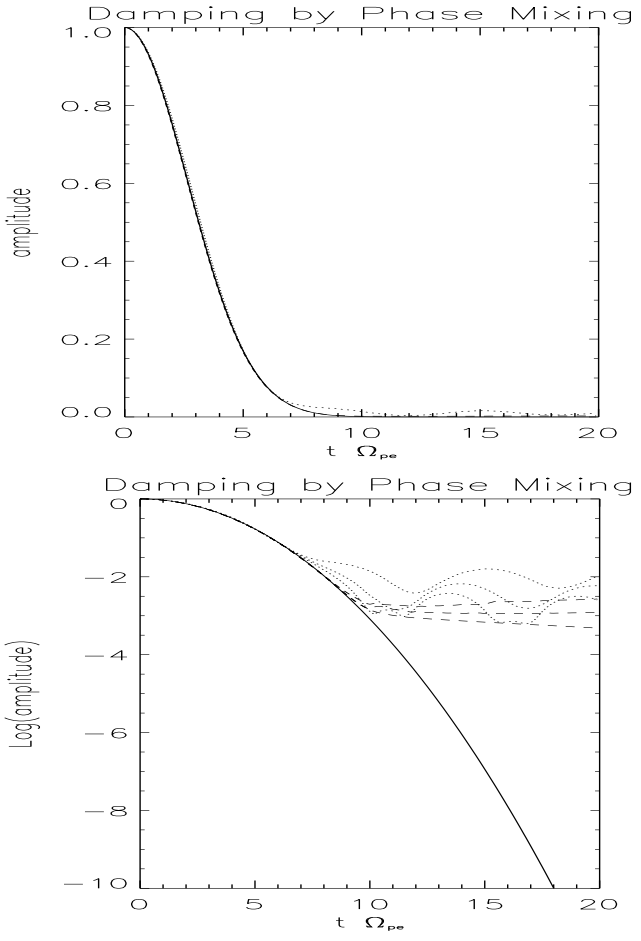

Fig. 3. Damping of inhomogenities by phase mixing. The solid line corresponds to the exact solution, the dotted lines to numerical solutions with $-3v_{Te} \leq v \leq 3v_{Te}$ ($nv = 20,\ 40,\ 80$ respectively) and the dashed lines to numerical solutions with $-10v_{Te} \leq v \leq 10v_{Te}$ ($nv = 66,\ 132,\ 264$ respectively). The lowest lines correspond to the highest velocity space resolution.

In Fig. 5 we compare these analytic results with numeric solutions. The solid lines correspond to the amplitude derived from our Vlasov code. ($L = 100\Lambda_{De}$, $v_{\max} = 10v_{Te}$, $nv = 132$, $nx = 400$, $k = 6, \epsilon = 0.01$)

The differences (error of $5 - 10\%$) in the analytic and numeric solutions are due to the fact that the limits for the validity of the analytic theory are fulfilled only very roughly.

$\frac{1}{kL}$	$k\Lambda_{De}$	$\frac{\Omega_r}{k\,v_{Te}}$	Ω_r num	Ω_r theo	Ω_i num	Ω_i theo
3	0.19	5.3	0.95	1.05	≈ 0	-10^{-5}
6	0.38	2.7	1.10	1.19	-0.110	-0.08
8	0.50	2.0	1.25	1.32	-0.17	-0.15

4 Null-helicity and co-helicity reconnection

The local structure of the reconnecting plasma is described with Harris sheet like current sheet. The pure Harris sheet

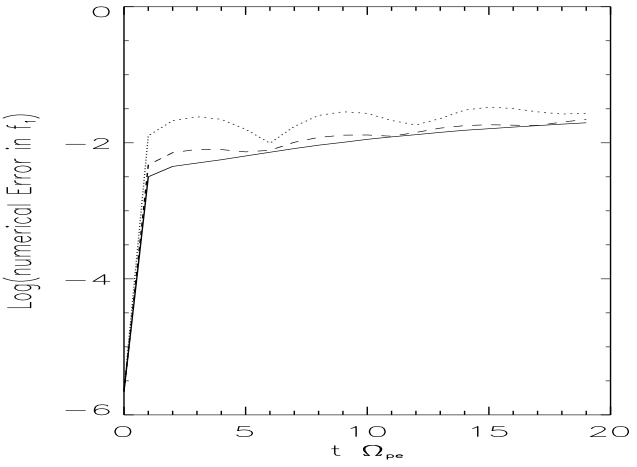

Fig. 4. Comparison of analytic and numeric solution for force free phase mixing. We plot $\ln(\sum_x \sum_v |f_{\text{analytic}} - f_{\text{numeric}}|)$ for different resolution and size of the velocity space (dotted line $v_{\max} = 3\,v_{Te}$, $nv = 20$, dashed line $v_{\max} = 3\,v_{Te}$, $nv = 80$, solid line $v_{\max} = 10\,v_{Te}$, $nv = 66$.

corresponds to a shear angle of reconnecting field lines of $180°$ and corresponds to reconnection at a neural line ($\boldsymbol{B} = 0$ reconnection, null-helicity reconnection). While a shear of exactly $180°$ is only a very special case, in general the angle between reconnecting field lines may be different to this strictly anti-parallel case. This more general case leads to magnetic reconnection at a magnetic field line ($\boldsymbol{B} \neq 0$ reconnection, co-helicity reconnection).

Null-helicity reconnection (or $\boldsymbol{B} = 0$ reconnection) occurs at a magnetic neutral line. In thin current sheets kinetic effects are important, because the limits of MHD break down. One important purely kinetic effect is the evolution of a perpendicular magnetic field. Due to the different mass of electrons and ions the mobility is different. Consequently the particle flux of ions and electrons out of the reconnection zone (X-point) is different. The ions are streaming mainly parallel to the x-axis, but the electrons along the separatrices of the magnetic field. The different particle flows cause Hall currents in the wings of the reconnected magnetic field around the X-point. Each of these currents in the xz-plane naturally causes a magnetic field B_y perpendicular to the reconnection plane. Due to the orientation of the Hall currents the perpendicular magnetic field B_y exhibits a quadrupolar structure. The quadrupolar structure of B_y causes a disortion of the reconnected magnetic field lines (see Wiegelmann and Büchner, 2001a, for details).

Co-helicity reconnection (or $\boldsymbol{B} \neq 0$ reconnection) occurs at a magnetic field line. Due to the existence of a magnetic field at the reconnection line the mobility of the electrons becomes reduced because the accelerated electrons become magnetized in the perpendicular magnetic field B_y. The accelerated electrons are trapped in this field and gyrate around the B_y direction. Thus the perpendicular magnetic field reduces the mobility of the electrons. Consequently the Hall

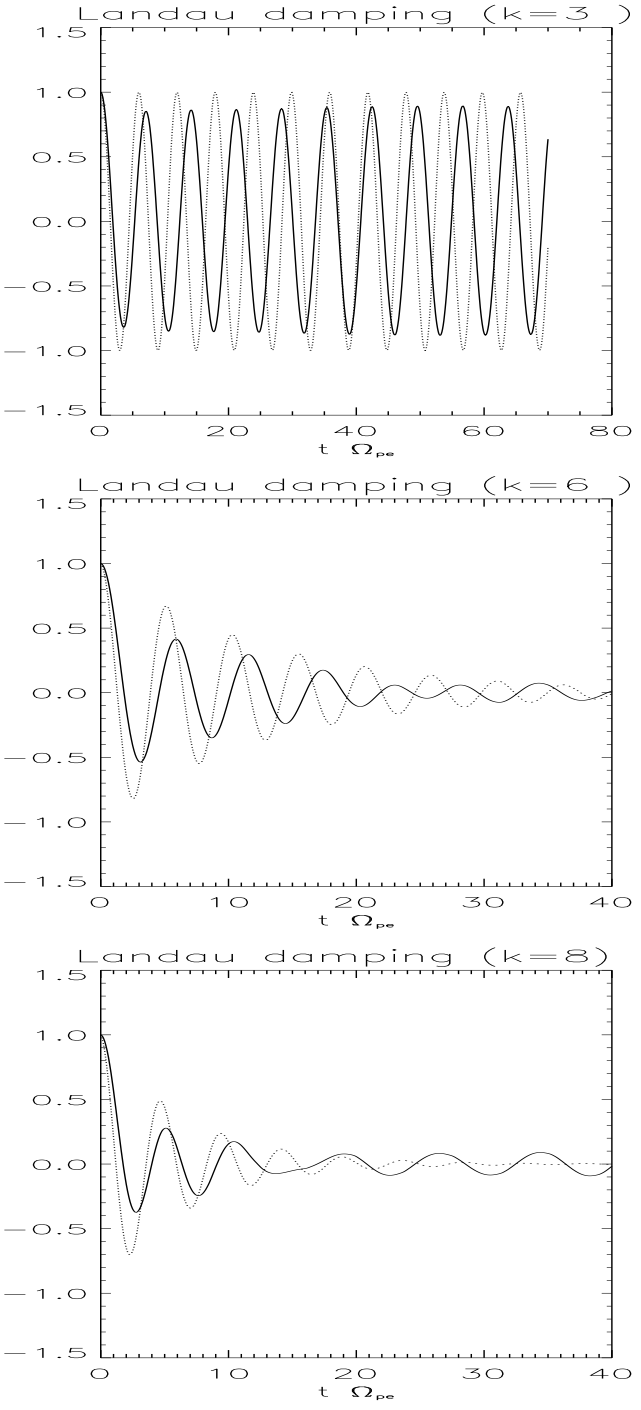

Fig. 5. Landau damping for different wavelength. The solid lines correspond to our numerical solutions and the dotted lines to the analytic solution.

currents, which occur in $\boldsymbol{B} = 0$ reconnection, do not occur for $\boldsymbol{B} \neq 0$ reconnection. One observes ring currents around the O-lines carried by the electrons. Due to these ring currents the magnetic field $B_y(x, z)$ becomes enhanced around the O-lines. This reconnected magnetic field gets a helical structure (see Wiegelmann and Büchner, 2001b, for details).

5 Conclusions

In this paper we presented tests and limits of Vlasov code simulations. Our results show that a finite velocity space leads to a less effective phase mixing, a process which is important for collisionless dissipation in plasmas and other collisionless multi particle systems. For a phase space limit of $3v_{Te}$ the error compared with exact theory is of the order of 10^{-2} and for $10v_{Te}$ of 10^{-4} which seems to be reasonable for most purposes. Due to the huge increase in required computer resources for $5D$ or $6D$ Vlasov code simulation one will, however, often have content with the error of 10^{-2} caused by the lower velocity space limits.

Acknowledgements. We thank Karl Schindler, Gunnar Hornig and Ilya Silin for useful discussions. This work was supported by PPARC.

References

Krall, N. A. and Trivelpiece, A. W., Principles of plasma physics, San Francisco Press, Inc., 1986.

Spatschek, K.H. Theoretische Plasmaphysik, B. G. Teubner, Stuttgart 1990.

Wiegelmann, T. and Büchner, J., Evolution of magnetic helicity in the course of kinetic magnetic reconnection, Nonlinear Processes in Geophysics, in press, 2001a.

Wiegelmann, T. and Büchner, J., Evolution of magnetic helicity under kinetic magnetic reconnection, Part II $\boldsymbol{B} \neq 0$ reconnection, Nonlinear Processes in Geophysics, accepted, 2001b.